HHS Public Access

Author manuscript

Mucosal Immunol. Author manuscript; available in PMC 2015 September 01.

Published in final edited form as:

Mucosal Immunol. 2015 March ; 8(2): 390–402. doi:10.1038/mi.2014.77.

IL-23 activates innate lymphoid cells to promote neonatal intestinal pathology

Lili Chen[#1], **Zhengxiang He**[#1], **Erik Slinger**[1], **Gerold Bongers**[1], **Taciana L.S. Lapenda**[1], **Michelle E. Pacer**[1], **Jingjing Jiao**[1], **Monique F. Beltrao**[1], **Alan J. Soto**[1], **Noam Harpaz**[2], **Ronald E. Gordon**[2], **Jordi C. Ochando**[1,3], **Mohamed Oukka**[4], **Alina Cornelia Iuga**[5], **Stephen W. Chensue**[6,7], **Julie Magarian Blander**[1], **Glaucia C. Furtado**[1], and **Sergio A. Lira**[1]

[1]Immunology Institute, Icahn School of Medicine at Mount Sinai, New York, NY 10029, USA

[2]Department of Pathology, Icahn School of Medicine at Mount Sinai, New York, NY 10029, USA

[3]Department of Nephrology, Icahn School of Medicine at Mount Sinai, New York, NY 10029, USA

[4]Department of Pediatrics, University of Washington, Seattle, WA 98101, USA

[5]Department of Pathology and Cell Biology, Columbia University Medical Center, New York, NY 10032, USA

[6]Department of Pathology, University of Michigan Medical School, Ann Arbor, MI 48105, USA

[7]Section of Pathology and Laboratory Medicine, Veterans Affairs Ann Arbor Healthcare System, Ann Arbor, MI 48105, USA

[#] These authors contributed equally to this work.

Abstract

Interleukin-23 (IL-23) responsive group 3 innate lymphoid cells (ILC3s) have been implicated in immune homeostasis and pathogenesis in the adult, but little is known about their roles in the newborn. Here we show that IL-23 promotes conversion of embryonic intestinal $Lin^{-}IL\text{-}23R^{+}Thy1^{+}$ cells into IL-22-producing $Thy1^{+}Sca\text{-}1^{hi}$ ILC3s *in vitro*. Gut-specific expression of IL-23 also activated and expanded $Thy1^{+}Sca\text{-}1^{hi}$ ILC3s, which produced IL-22, IL-17, IFN-γ, and GM-CSF and were distinct from canonical $CD4^{+}$ lymphoid tissue inducer (LTi) cells. These ILC3s accumulated under the epithelium in intercellular adhesion molecule (ICAM)-1 positive cell aggregates together with neutrophils that disrupted the epithelium, leading to the formation of discrete intestinal erosions, bleeding, and neonatal death. Genetic and antibody depletion of ILC3s rescued the mice from neonatal death. Antibiotic treatment of pregnant mothers and offspring prolonged survival of IL-23 transgenic mice, suggesting a role for the commensal flora on ILC3-induced pathogenesis. Our results reveal a novel role for the IL-23-ILC3s axis in the pathogenesis of neonatal intestinal inflammation.

Correspondence: Sergio A Lira, phone: 212-659-9404; fax: 212-849-2525; sergio.lira@mssm.edu)..

Disclosure:
The authors declare no conflict of interest.

Introduction

Interleukin-23 (IL-23) is a heterodimeric cytokine formed by the IL-23-specific p19 subunit and the IL-12p40 subunit[1]. IL-23 plays a pivotal role in adult intestinal inflammation[2]. Recent evidence suggests that IL-23 acts as a molecular switch to promote pathological T cell and innate lymphoid cell (ILC) responses in murine models of colitis and in human inflammatory bowel disease (IBD) [3-9].

ILCs regulate immunity, inflammation, tissue repair and remodeling in multiple anatomical compartments, particularly at mucosal surfaces[10]. ILCs are currently categorized into three distinct populations based on their developmental requirements for defined transcription factors, expression of cell surface markers, and secretion of specific cytokines [11-13]. IL-23 has been implicated in the activation and induction of group 3 ILCs (ILC3s) [13]. ILC3s depend on the transcription factor RORγt and are also called RORγt$^+$ ILCs. ILC3s can be further categorized into several subsets with distinct but overlapping phenotypic and functional markers. Lymphoid tissue inducer (LTi) cells represent the subset of ILC3s responsible for the formation of secondary lymphoid organs during embryogenesis[14, 15]. Intestinal LTi cells do not generally express lineage-specific markers but can express the T cell surface molecule CD4[16, 17]. Two other subsets of group 3 ILCs are defined by their expression of natural cytotoxicity receptors (NCRs, including NKp46 and NKp44) and are thus categorized into NCR$^+$ILC3s and NCR$^-$ILC3s[12, 13]. NCR$^+$ILC3s also play a role in gut-associated lymphoid tissue generation[18, 19], and appear to be essential for host protective immunity in the intestine[20]. The development/maintenance of NCR$^+$ILC3s, different from LTi cells, appears to be dependent of commensal-derived signals[21-23]. Another subset within the group 3 ILCs was found to mediate pathology in a mouse model of innate colitis[4]. These colitogenic NCR$^-$ILC3s lack expression of NKp46 and do express thymocyte differentiation antigen 1 (Thy1), stem cell antigen 1 (Sca-1) and IL-23 receptor (IL-23R) and secrete both IFN-γ and IL-17 in addition to IL-22 under IL-23 stimulation [4]. These NCR$^-$ILC3s accumulate in the inflamed colon and are directly responsible for the chronic pathology.

While it is established that IL-23 affects both the maintenance of a Th17 response [3, 8] and activation and function of group 3 ILC3 in adults[12], little is know about its role in early development. It is generally accepted that the immune system is immature at birth because the structure of bone marrow, spleen, and lymphoid nodes is not fully defined, there are few B and T cells in circulation and in the periphery, and there are no memory B and T cells [24-26]. However, some aspects of the immune response are already in place. For instance, human neonatal dendritic cells (DCs), respond to Toll-like receptor (TLR) stimulation by secreting large amounts of IL-23 [27-29]. Human neonatal DC-derived IL-23 promotes the differentiation of neonatal CD8$^+$ T cells into IL-17-producing cells [30]. In addition, human neonatal DC-derived IL-23 combined with specific TCR signaling drives the generation of neonatal γδT cells equipped with a range of cytotoxic mediators and distinct subpopulations producing IFN-γ and IL-17 [25]. Isolated DCs from neonatal mice are able to produce relatively higher levels of IL-23p40, but lower levels of IL-12p70 than their DC counterparts in adult mice[31, 32].

Here we show that IL-23 promotes differentiation of embryonic Thy1$^+$IL-23R$^+$ intestinal cells into Thy1$^+$Sca-1^{hi} ILC3s *in vitro*. Gut-specific expression of IL-23 in transgenic mice promoted significant expansion of a subset of ILC3s that together with neutrophils and the intestinal flora promoted development of erosive lesions, bleeding and neonatal death. These results indicate that increased IL-23 expression can promote development of pathogenic ILC3s in the newborn intestine.

Results

IL-23 activates embryonic IL-23R$^+$Thy1$^+$ cells to become IL-22-producing RORγt$^+$Thy1$^+$Sca-1^{hi} cells *in vitro*

While a role for IL-23 in regulating immune homeostasis and pathogenesis in the adult is firmly established [3, 13], its role in the prenatal/neonatal immune regulation is poorly understood. To start studying the role of IL-23 in this period, we examined the distribution of IL-23 responsive cells in the intestine. IL-23 interacts with cells that co-express the IL-23R subunit and the shared IL-12R β1 chain [33]. We took advantage of IL-23R green fluorescent protein (GFP) reporter mice[34] to determine which cells expressed IL-23R. Most (~70%) CD45$^+$ IL-23RGFP$^+$ cells in the gut of prenatal mice were lineage-negative (Lin$^-$) cells. The remaining cells were CD11b$^+$ (~18%) and CD11c$^+$ (~12 %) (Supplementary fig. S1). Most Lin$^-$ IL-23RGFP$^+$ cells (80%) were Thy1$^+$Sca-1$^-$ cells in the intestine of *Il-23r*$^{+/gfp}$ mice at embryonic day E18.5 (Fig. 1a). Culture of embryonic leukocytes from the *Il-23r*$^{+/+}$ intestine with recombinant IL-23 promoted development of Lin$^-$Thy1$^+$Sca-1^{hi} cells (Fig. 1b). Incubation of intestinal cells from IL-23R-deficient (*Il-23r*$^{gfp/gfp}$) embryos with IL-23, as expected, did not result in the appearance of Lin$^-$Thy1$^+$Sca-1^{hi} cells (Fig. 1b). Further characterization of this IL-23 stimulated Lin$^-$Thy1$^+$Sca-1^{hi} cell population showed that they were negative for CD4, NKp46, and CCR6 (Supplementary fig. S2). Adult IL-23-responsive cells produce IL-17 and/or IL-22 when challenged with IL-23 [13]. Lin$^-$Thy1$^+$Sca-1^{hi} cells generated *in vitro* after stimulation with IL-23 produced IL-22 (Fig. 1c), but not IL-17.

To further confirm that IL-23 acted directly on the Lin$^-$Thy1$^+$ cells, we sorted Lin-Thy1$^+$ and Lin$^-$Thy1$^-$ cells from the intestine of embryonic wild-type (WT) mice and cultured them in the presence of IL-23 or vehicle. We found that the Lin$^-$Thy1$^+$ cells converted to Lin$^-$Thy1$^+$Sca-1^{hi} cells after IL-23 stimulation (Fig. 1d). As CD3$^-$CD4$^+$ LTi cells are also Thy1$^+$ [13], we asked next whether Lin$^-$Thy1$^+$IL-23R$^+$CD4$^-$ cells could respond to IL-23. We sorted Lin$^-$Thy1$^+$IL-23R$^+$CD4$^-$ cells from the intestine of *Il-23r*$^{+/gfp}$ mice and challenged them with IL-23. We found that more than 90% of the Lin$^-$Thy1$^+$IL-23R$^+$CD4$^-$cells became Lin$^-$Thy1$^+$Sca-1^{hi} cells (Fig. 1e).

To further gain insight into how IL-23 promoted the development of Lin$^-$Thy1$^+$Sca-1^{hi} cells, we examined expression of RORγt and IL-22 . Treatment of the Lin$^-$Thy1$^+$ IL-23R$^+$ CD4$^-$ cells with IL-23 increased expression of *Rorc* (Fig. 1f) and *Il-22* (Fig. 1f and g). Incubation of intestinal cells from RORγt-deficient embryos with IL-23, as expected, did not result in the appearance of Lin$^-$Thy1$^+$Sca-1^{hi} cells (Supplementary fig. S3), suggesting that RORγt is critical for Lin$^-$Thy1$^+$Sca-1^{hi} cells development. Together, these results indicate

that IL-23 activates embryonic Lin^{-}IL-23R^{+}Thy1^{+} cells to become IL-22-producing RORγt^{+}Thy1^{+}Sca-1^{hi} group 3 ILCs *in vitro*.

Transgenic expression of IL-23 in the neonatal intestine causes erosive lesions, bleeding and neonatal death

To study if IL-23 had a role in the activation of ILC3s in the intestine, we generated IL-23 transgenic mice. To do so, we first developed sets of mice expressing IL-23p19 *(V19* mice) and IL-23p40 (*V40* mice) from the villin promoter, which targets expression of transgenes to the intestinal epithelium[35]. *V19* and *V40* mice were then intercrossed to generate *V23* mice (Fig. 2a). Surprisingly, no *V23* transgenic mice were found alive at postnatal day 8 (P8) (Fig. 2b), suggesting early mortality. Further genotypic analysis showed that *V23* mice survived gestation but died at P0-P1 (Fig. 2b). To confirm transgene expression, we performed enzyme linked immunosorbent assay (ELISA) in gut extracts and found that IL-23 levels were ~ 7 fold higher in the intestine of transgenic mice than controls (Supplementary fig. S4). These levels are comparable to those induced by administration of CD40-specific antibodies to activate IL-23 expression in Rag$^{-/-}$ mice [36].

Further examination of abdominal organs revealed that the small intestine was prominently affected in the transgenic mice (Fig. 2c). On gross examination, the *V23* mice had congested and dilated small bowels compared with littermate WT control mice (Fig. 2c). Histologically, the general architecture of the intestine was preserved, but the lumen appeared distended and showed hemorrhage (Fig. 2c). The most distinguished finding was the presence of discrete epithelial lesions overlying lamina propria lymphoid aggregates (Fig. 2d). The lesions consisted of disrupted epithelium in association with intraepithelial and superficial subepithelial neutrophilic infiltrates (Fig. 2d). Neutrophils were also seen in the intestinal lumen, at the sites of epithelial disruption (Fig. 2d). Scattered epithelial apoptotic bodies and reactive/regenerative epithelial changes were also seen at the site of the lesions (Fig. 2, c and d).

To further ascertain that the biology observed was dependent on IL-23, and to rule out the possibility that the early lethality in the *V23* mice could be a consequence of a non-specific effect caused by expression of two independent transgenes (Fig. 2, a and b), we intercrossed the *V19* and *V40* to mice deficient in the IL-23R (*Il-23r*$^{GFP/GFP}$) to generate *V23 Il-23r*$^{GFP/GFP}$ mice. Similar to *V23* mice, *V23 Il-23r*$^{+/GFP}$ mice succumbed immediately after birth. In great contrast, *V23 Il-23r*$^{GFP/GFP}$ mice survived to adulthood and did not show any signs of disease (Fig. 2, e and f). These results indicate that the phenotype observed in the *V23* mice is directly elicited by the interaction of IL-23 with its receptor, and not the consequence of a spurious artifact induced by expression of the transgenes.

IL-23 expression drives expansion of intestinal Lin^{-}Thy1^{+}Sca-1^{hi} cells in mice

Next we asked whether transgenic expression of IL-23 *in vivo* affected development of Lin^{-}Thy1^{+}Sca-1^{hi} ILCs in the neonatal intestine. First we examined the frequency of Lin-Thy1^{+}Sca-1^{hi} population in the different organs of *V23* transgenic mice at P0. IL-23-responsive Lin^{-}Thy1^{+}Sca-1^{hi} cells were most abundant in the small intestine (SI), representing 40-50% of all Lin^{-} population, but were also present in the large intestine (LI),

mesenteric lymph nodes (MLN), and at lower frequency in the spleen (Fig. 3a). In contrast, no Lin$^-$Thy1$^+$Sca-1^{hi} cells were detected in the intestine, MLN or spleen of WT mice (Fig. 3a). The total number of Lin$^-$Thy1$^+$Sca-1^{hi} cells in the SI of transgenic mice was dramatically increased compared to that of WT mice (Fig. 3b).

At birth the relative and absolute number of leukocytes (CD45$^+$ cells) in the small intestine *V23* mice was increased (Fig. 3c). The most increased leukocytes in Lin$^+$ population were CD11b$^+$ cells (Fig. 3, d and e). The dominant population among the CD11b$^+$ cells were neutrophils (CD11b$^+$MHCII$^-$Gr-1$^+$ cells), whose numbers were markedly increased in the intestine of *V23* mice compared with WT mice (Fig. 3f). Further analyses showed that there were no changes in the relative number of most leukocytes (Fig. 3d), with only modest increases in the absolute number of CD3$^+$ cells, B220$^+$ cells, and CD11c$^+$ cells in *V23* mice compared to WT mice (Fig. 3e). As expected, Thy1$^+$Sca-1^{hi} cells were the most abundant Lin$^-$ cells (Fig. 3, b, d and e). Other CD45$^+$ Lin$^-$ cells such as the canonical intestinal LTi cells (Lin$^-$CD4$^+$) were decreased in *V23* mice compared with WT mice (Fig. 3g). In addition, no NKp46$^+$ILC3s were detected in transgenic nor WT mice at this stage, consistent with the fact that NKp46$^+$ILC3s develop several days after birth and are normally induced by the intestinal commensal flora [21, 23].

Together these results indicate that IL-23 expression promoted the expansion of a distinct set of Thy1$^+$Sca-1^{hi} ILCs and increased in the numbers of neutrophils in the small intestine of *V23* neonates.

Lin$^-$Thy1$^+$Sca-1^{hi} cells present in the intestine of the *V23* mice are NCR$^-$ILC3s

To characterize the Lin$^-$Thy1$^+$Sca-1^{hi} cells further, we examined expression of surface markers, transcription factors, and cytokines by flow cytometry. The Lin$^-$Thy1$^+$Sca-1^{hi} cells present in the neonatal small intestine of *V23* mice coexpressed markers normally associated with ILC3s, such as IL-23R, RORγt, IL-7R (CD127), CD44, CD25, c-Kit (CD117) and CCR6 (Fig. 4a). Lin$^-$Thy1$^+$Sca-1^{hi} cells did not express CD4 or NKp46 (Fig. 4a) but did express high levels of Sca-1, which suggests that they were phenotypically distinct from LTi cells and NKp46$^+$ILC3s [12, 13]. Further phenotypic analysis showed that IL-18R and cytotoxic T-lymphocyte antigen 4 (CTLA-4) were expressed in Lin$^-$Thy1$^+$Sca-1^{hi} cells (Fig. 4a). Interestingly, CTLA-4 was expressed by Lin$^-$Thy1$^+$Sca-1^{hi} cells but not by classical LTi cells (Fig. 4a). Similar to human LTi-like ILCs [37], Lin$^-$Thy1$^+$Sca-1^{hi} cells expressed TLR2 (Fig. 4a) .

IL-22, IL-17 and IFN-γ are produced not only by Lin$^+$ cells, such as Th17 cells and γδT cells, but also by mucosal ILCs. Intracellular flow cytometry revealed that neonatal CD45$^+$Lin$^-$ cells, but not Lin$^+$ cells, produced most of IL-22, IL-17, IFN-γ and granulocyte-macrophage colony-stimulating factor (GM-CSF) in the intestine of *V23* mice (Fig. 4b), which is consistent with the fact that very few CD3$^+$ cells were present at this stage in the intestine (Fig. 3, d and e). Further analysis showed that most of these cytokines (IL-22, IL-17, IFN-γ and GM-CSF) were produced by Lin$^-$Thy1$^+$Sca-1^{hi} ILCs (Fig. 4c). The vast majority (80-95%) of Thy1$^+$Sca-1^{hi} ILCs produced IL-22 (Supplementary fig. S5a). Approximately 30% of the Thy1$^+$Sca-1^{hi} ILCs produced only IL-22 and the remaining cells co-expressed it with IL-17, IFN- γ or GM-CSF (Supplementary fig. S5a). Of note, we

observed that ~6% of the cytokine expressing cells, expressed IL-22, IL-17, IFN-γ and GM-CSF (Supplementary fig. S5b). Together these results indicate that the distinct Thy1^{+}Sca-1^{hi} ILC population present in the neonatal intestine of *V23* transgenic mice most closely resembles the NCR-negative group 3 ILCs reported in adult host [4, 5].

ILC3s and neutrophils co-localize in cellular aggregates beneath the intestinal erosive lesions

Having detected the presence of Thy1^{+}Sca-1^{hi} ILC3s in the small intestine of *V23* mice, we investigated next their distribution. To do so, we first performed anti-Thy1 immunostaining. We found Thy1^{+} cells in the erosive lesions, but not in adjacent areas (Fig. 5a). These cells were interspersed among cells expressing the intercellular adhesion molecule (ICAM)-1, which is commonly expressed within lymph nodes and Peyer's patches (PP) anlagen (Fig. 5a). To further confirm the presence of cytokine-producing cells in these areas, we performed laser-capture microdissection of the erosive lesions and the adjacent areas of the intestine of *V23* mice, extracted mRNA and performed quantitative RT-PCR analysis for cytokines (Fig. 5b). As control, we investigated cytokine mRNA expression in samples collected from PP's anlagen and adjacent areas of WT mice (Fig. 5b). Quantitative RT-PCR results showed that with the exception of IL-17, no cytokines were expressed in PP of WT mice at this point (Fig. 5c). In contrast, IL-22, IL-17, IFN-γ and GM-CSF mRNA were all expressed in the areas corresponding to the erosive lesions of *V23* mice compared to all other microdissected samples (Fig. 5c), suggesting that cytokine-producing ILC3s clustered in the erosive lesions. IL-22 immunofluorescence staining subsequently confirmed that cells expressing IL-22 localized to cell clusters under the erosive lesions in the small intestine of *V23* mice (Fig. 5d).

Besides expressing cytokines, ILC3s express chemokine receptors such as CXCR5 (Supplementary fig. S6) and CCR6 (Fig. 4a). We tested next if the presence of ILC3s in the erosive lesions was associated with increased expression of CXCL13 and CCL20, ligands for CXCR5 and CCR6 respectively. In the WT intestine CXCL13, along with CCL19 and CCL21, is expressed constitutively in PP[38-40]. Consistent with these previous findings, we detected increased expression of *Ccl19*, *Ccl21* and *Cxcl13* within ICAM-1^{+} PP anlagen of P0 WT mice (Fig. 5e). In *V23* mice, expression of ICAM-1 localized to the erosive lesions, and increased levels of *Cxcl13* mRNA were detected compared to neighboring areas (Fig. 5e). *Ccl19* and *Ccl21* mRNA levels did not differ between erosive and adjacent areas (Fig. 5e). *Ccl20* mRNA was only modestly increased in PP of controls and did not differ between erosive and adjacent areas of *V23* intestine (Fig. 5e). These results suggest that CXCL13 may be important for recruitment of ILC3s into the ICAM-1^{+} erosive areas of the *V23* intestine.

Because neutrophil numbers were also increased in the small intestine of *V23* mice (Fig. 3f), we examined next their distribution. Neutrophils were abundant in the same areas where ILC3s were found (Fig. 5f). Ultrastructural analysis showed that neutrophils migrated from the lamina propria to the lumen and disrupted the epithelium (Supplementary fig. S7), leading to formation of the erosive lesions. Of note, we found that cells isolated from the erosive lesions in *V23* mice expressed higher levels of neutrophil-recruiting chemokines

Cxcl1, *Cxcl2* and *Cxcl7* than those from adjacent control areas or from PP anlagen of WT mice (Fig. 5g).

Together the data indicate that ILC3s and neutrophils co-localize in cellular aggregates beneath the intestinal erosive lesions, and suggest that specific chemokines may be involved in their recruitment to those sites.

Thy1^{+}Sca-1^{hi} ILCs contribute to neonatal intestinal pathology

IL-23-responsive NCR^{-}ILC3s mediate intestinal immune pathology in adult murine models of colitis [4, 6]. To test if the Thy1^{+}Sca-1^{hi} ILC3s could contribute to the neonatal pathology observed in the *V23* mice, we first injected an anti-Thy1 mAb into pregnant mice and newborn pups and estimated the frequency of Thy1^{+}Sca-1^{hi} ILCs in their offspring at P4 (Fig. 6a). Anti-Thy1 mAb injection reduced the total number of Thy1^{+}Sca-1^{hi} cells in *V23* mice (Fig. 6b). These animals had fewer erosive lesions in the intestine (Supplementary fig. S8a) and survived longer than the *V23* mice treated with isotype control antibodies (Fig. 6c).

To genetically deplete the ILC3 population we intercrossed the *V19* and *V40* mice to mice deficient in the *Rorc* to generate *V23Rorc* $^{-/-}$ mice. RORγt deficient mice lack all ILC3s [12]. At birth, *V23 Rorc* $^{+/-}$ mice had fewer Thy1^{+}Sca-1^{hi} ILC3s than *V23* mice (Fig. 6d) and survived longer than *V23* mice (Fig. 6e). As expected, *V23 Rorc* $^{-/-}$ mice did not have Thy1^{+}Sca-1^{hi} ILCs (Fig. 6d) and survived to adulthood (Fig. 6e). Accordingly, there were no erosive lesions present in the intestine of *V23 Rorc* $^{-/-}$ mice (Supplementary fig. S8b) consistent with the fact that RORγt deficient mice lack Peyer's patches[41]. Similar to *V23 Rorc* $^{-/-}$ mice, no Thy1^{+}Sca-1^{hi} ILCs were present in *V23 Il-23r* $^{gfp/gfp}$ mice (Supplementary fig. S9) that survived to adulthood (Fig. 2f).

At birth, few T cells are present in the intestine (Fig 3, d and e). To rule out a contribution of T cells to the phenotype observed in *V23* mice, we intercrossed the *V19* and *V40* mice to *RAG1*$^{-/-}$ mice and to mice deficient in the gamma delta T-cell receptor (*Tcrd*$^{-/-}$) to generate *V23 RAG1*$^{-/-}$ and *V23 Tcrd*$^{-/-}$ mice respectively. *V23 RAG1*$^{-/-}$ and *V23 Tcrd*$^{-/-}$ mice succumbed immediately after birth and presented erosive lesions (Supplementary fig. S10) similar to those noted in *V23* mice (Fig 2d and Supplementary fig. S10). Together these results indicate that Thy1^{+}Sca-1^{hi} ILC3s, but not T and B cells, have a critical role in neonatal intestinal pathology and perinatal death of *V23* mice.

Intestinal embryonic Thy1^{+}Sca-1^{hi} ILC3s dysregulate epithelial permeability

We examined next whether the NCR^{-}ILC3s were present during the prenatal stage. We found that Thy1^{+}Sca-1^{hi} ILC3s were present in the *V23*, but not WT fetuses, prior to birth (Fig. 7a) and that the relative number of these cells was not different between late fetal stages and birth (Figs. 3a and 7a). As some studies indicate that commensal-derived signals may also contribute to ILCs function[22, 42], we analyzed next the cytokine production by Thy1^{+}Sca-1^{hi} ILC3s in prenatal period. We found that fetal Thy1^{+}Sca-1^{hi} ILC3s (Fig. 7b) expressed IL-22, IL-17, IFN-γ and GM-CSF similar to the postnatal Thy1^{+}Sca-1^{hi} ILC3s (Fig. 4c).

Given that cytokine-producing Thy1^{+}Sca-1^{hi} ILC3s could be found in the embryonic gut, we asked next if they could promote prenatal pathology. Histopathological analysis of the intestine of *V23* fetuses at E18.5 showed no epithelial disruption or intestinal bleeding, but revealed the presence of cellular aggregates with few scattered subepithelial neutrophils (Fig. 7c). Quantitative RT-PCR analysis of sorted epithelial cells of *V23* mice revealed that *epcam*, *cldn*1, 2, 3, 7 and *cdh1* expression was downregulated in *V23* mice compared to controls (Supplementary fig. S11). These results suggested a possible dysfunction in epithelial permeability. To test this hypothesis we injected the intestinal lumen of E18.5 *V23* and WT embryos with sulfo-NHS-biotin, a probe that labels cell membrane proteins [43]. As control, we examined the biotin signal at the intestinal epithelium of WT mice. The intestine of the WT mouse was uniformly labeled, with no dye being detected in the lamina propria (Fig. 7d). The intensity of the biotin signal in areas of the lamina propria, especially in the area corresponding to the cellular aggregates, was higher in the *V23* mice than in WT mice (Fig. 7d and e), suggesting increased permeability of the epithelium at those sites. We also examined, as an additional control, the intestine of *V23 Il-23r*$^{gfp/gfp}$ mice injected with sulfo-NHS-biotin. The results were similar to those obtained with WT mice (Fig. 7d), which ruled out the possibility that the dysregulated intestinal epithelial permeability in the *V23* mice resulted from a transgenic artifact.

Together the findings indicate that *V23* mice had downregulation in the expression of genes involved in maintaining the epithelial barrier, and increased permeability of the epithelium in areas rich in cytokine-producing NCR^{-}Thy1^{+}Sca-1^{hi} ILC3s.

Commensal bacteria aggravate intestinal pathology induced by Thy1^{+}Sca-1^{hi} ILCs after birth

As demonstrated above, cytokine-producing ILC3s were present in the embryonic *V23* intestine and their presence was associated with increased epithelial permeability. Yet, no significant damage or mortality was observed in embryos, suggesting that ILC3s were necessary, but not sufficient to induce the full phenotype. We next tested the hypothesis that the microbiota could contribute to the neonatal phenotype. Bacterial colonization of the newborn intestinal tract starts as the fetuses pass the birth canal and continues with the initial feeding and exposure to the environment. We thus tested if there were differences in the initial colonization of the intestine between WT and *V23* mice. We subjected DNA collected from the small intestine of P0 *V23* and WT littermate controls to 16S rDNA sequencing. Weighted UniFrac distances (PC1, $P = 0.82$; Supplementary fig. S12a) and alpha diversity analysis ($P > 0.9$, Supplementary fig. S12b) indicated that the microbiota of *V23* mice was similar to that of WT littermate controls. Analysis of the most abundant phyla did not indicate any major changes in the relative abundance between *V23* and WT littermate controls (Supplementary fig. S12c). In total, 156 individual OTUs were retained after quality filtering, none of which showed a significant difference between *V23* and WT mice ($q > 0.05$, Supplementary fig. S12d).

Having demonstrated that the expression of IL-23 and increased numbers of ILC3s did not affect the initial bacterial colonization of the gut, we tested next if a reduction of the bacterial load would affect the phenotype. To reduce the exposure of newborn *V23* mice to

bacteria, we treated pregnant mothers with antibiotics. Antibiotic treatment prolonged the survival and decreased the number of intestinal erosive lesions in the newborn *V23* mice (Fig. 8, a and b), implicating the microbiota in ILC3s-induced pathogenesis. Of note, we found a reduced neutrophil infiltrate in the intestine of antibiotic-treated *V23* mice (Fig. 8c), suggesting that neutrophil accumulation in the ulcers could be due in part to the intestinal bacterial colonization.

We next examined if bacteria affected the phenotype by affecting the number or activity of ILC3s. There were no significant differences in the number of Thy1^{+}Sca-1^{hi} ILC3s between antibiotic treated and untreated *V23* mice (Fig. 8, d and e). We then examined gene expression in highly purified intestinal Thy1^{+}Sca-1^{hi} ILC3s from non-treated, and antibiotic-treated neonatal *V23* mice. No significant differences were observed in the expression of surface markers (Il23r, Kit, Cd44, Cxcr5, Ccr6, Il18r1, Ctla4, et al.) or cytokines (*Il22*, *Il17a*, *Ifng* and *Csf2*) (Supplementary fig. S13) between these two groups. The expression of ILC3s signature cytokine genes was also similar between non-antibiotic treated fetal and postnatal Thy1^{+}Sca-1^{hi} ILC3s (Supplementary fig. S13), corroborating the results reported above (Fig. 4c and 7 a, b).

These results indicated that Thy1^{+}Sca-1^{hi} ILC3s were necessary but not sufficient for the neonatal intestinal pathology observed in *V23* mice. Bacterial colonization at birth exacerbates pathology induced by these cells and promotes neonatal death.

Discussion

Most studies to date have examined IL-23 biology during the course of bacterial infections and/or gastrointestinal tract injury in the adult host, but a direct role for IL-23 in the activation and function of neonatal ILC3s has not yet been investigated. Results shown in the present study indicate that dysregulated expression of IL-23 during the immediate neonatal period promotes development of a population of innate lymphoid cells with pathogenic properties.

At birth the mouse intestine is populated by few T cells (Fig. 3, d and e), but is home to myeloid cells and innate lymphoid cells that express the IL-23 receptor[2, 12, 13]. Here, we have used *in vitro* approaches (Fig. 1) and reductionist genetic models (Fig. 2) to examine the contribution of IL-23 to the activation and function of these IL-23R^{+} ILC3s. Using an *in vitro* culture system, we demonstrated that IL-23 directly promoted development of IL-22-producing Thy1^{+}Sca-1^{hi} ILC3s. We also show that gut-specific expression of IL-23 expanded this population in the neonatal intestine. Together these results indicate that expression of IL-23 promotes development and function of Thy1^{+}Sca-1^{hi} ILC3s in the neonatal intestine. These neonatal Thy1^{+}Sca-1^{hi} ILC3s (Fig. 4) shared similarities with a NCR^{-}ILC3 population found in the adult colon by other groups [4, 6]. Neonatal Thy1^{+}Sca-1^{hi} NCR^{-}ILC3s concentrated in the small intestine and were found in clusters with ICAM^{+} cells and neutrophils in areas that resembled Peyer's patches anlagen (Fig. 5). Thy1^{+}Sca-1^{hi} NCR^{-}ILC3s expressed LTi-related genes such as LT-α, LT-β, and TRANCE [4], but were not canonical LTis, because they did not express CD4 (Fig. 4a). However, similar to LTi, Thy1^{+}Sca-1^{hi} NCR^{-}ILC3s expressed IL23R and the chemokine receptor CXCR5, which is

responsive to CXCL13, a chemokine expressed in lymphoid anlagen. The fact that these two cell populations express many similar markers and are located in the same intestinal area suggests that they may share a common developmental origin. It remains to be tested if IL-23 stimulates further differentiation of LTi into pathogenic Thy1^{+}Sca-1^{hi} NCR^{-}ILC3s or whether it acts on a common precursor that is recruited into the anlagen.

There appears to be significant heterogeneity within group 3 ILCs in the adult intestine. Some ILC3s are predominantly IL-22 producers, some primarily produce IL-17, while others can produce IFN-γ [4, 6, 44]. It is unclear if these represent different subsets of cells, or if this reflects different cytokine expression profiles in response to environmental signals. In a murine model of *Helicobacter hepaticus*-mediated colitis, RORγt^{+} ILCs in the colon produce IL-17A and IFN-γ and depletion of these cells prevents colitis[4]. ILC3s secreting IL-17A, but little IFN-γ, have also been implicated in the pathogenesis of the *Tbx21*$^{-/-}$*Rag2*$^{-/-}$ ulcerative colitis (TRUC) disease model. Treatment with a Thy1-specific antibody also ameliorates disease in this setting[6]. Here we show that IL-23 induced Thy1^{+}Sca-1^{hi} ILCs express only IL-22 *in vitro* (Fig. 1g). *In vivo*, the Thy1^{+}Sca-1^{hi} ILCs induced by IL-23 produce several cytokines, including IL-17, IL-22, IFN-γ, and GM-CSF (Fig. 4c). Most cells produced IL-22 and IL-17, but cells expressing different combinations of cytokines, or even all cytokines simultaneously, were also identified. To our knowledge, the existence of a population expressing all these cytokines simultaneously has not been previously demonstrated.

Our results indicate that increased IL-23 signaling in the immature, early intestine, led to an exaggerated generation of NCR^{-}ILC3s, and to uncontrolled production of cytokines. These ILC3s are likely to be the main drivers of the pathogenesis because they were the main cytokine producers. The few T cells present at this stage did not produce cytokines, nor do the γ δ T cells or other Lin^{+}/Lin^{-} populations. Furthermore, reduction or ablation of NCR^{-}ILC3, but not T and B cells (Supplementary fig. S10), reduced or eliminated disease, suggesting that this population is critical for pathogenesis in the neonatal gut.

Group 3 ILCs include LTi cells, NCR^{+}ILC3s and NCR^{-}ILC3s[13]. LTi cells develop in the microbiota-free environment of the fetus before birth[14, 15], whereas NKp46^{+} RORγ t^{+} ILC3s only appear after birth and are not found in embryonic mice [21, 23]. Thy1^{+}Sca-1^{hi} ILC3s were present in the *V23* fetal intestine (Fig. 7a), but did not appear to cause pathology, suggesting that they were necessary, but not sufficient to cause disease. Results shown here indicate that antibiotic-treatment of pregnant mothers prolonged survival of *V23* offspring (Fig. 8a), suggesting that commensal bacterial-derived signals affected the pathology induced by Thy1^{+}Sca-1^{hi} ILC3s. Despite being localized near barrier surfaces populated by commensal flora[45], ILC3s did not affect the initial bacterial colonization of the intestine (Supplementary fig. S12). Bacterial colonization did not affect the numbers of ILC3s or the expression of signature cytokines by these cells (Fig. 8e and Supplementary fig. S13). Our results suggest that ILC3s induced pathology by altering barrier integrity (Fig. 7d and Supplementary fig. S11). Penetration of bacteria or bacterial products through areas of ILC3-induced increased permeability located in the anlagen, could lead to uncontrolled bacterial proliferation, cytokine storm and death.

Our findings may have relevance for understanding the development of intestinal inflammatory diseases of the neonate. The fetus and young infant have a high susceptibility to infections with pathogens, suggesting that immune responses are different in early life [46]. It is generally accepted that this increased susceptibility is related to the immaturity/deficiencies of the neonatal immune system. However, there is evidence that some responses rather than inhibited, are exaggerated. For instance, human neonatal dendritic cells, respond to Toll-like receptor stimulation by secreting large amounts of IL-23 [27-29]. Robust expression of IL-23 by DC after bacterial exposure could trigger development and activation of ILC3 in the neonatal gut and lead to disease. In this context, it is important to note that IL-23 expression has been detected in the neonatal ileum of experimental models of necrotizing enterocolitis (NEC) [47]. NEC is the most common inflammatory disease of the gastrointestinal tract of preterm infants [48]. The etiology of NEC is obscure, but the disease is characterized by intestinal bleeding, mucosal intestinal necrosis and bacterial translocation. Increased bacterial translocation could trigger IL-23 production and expansion of pathogenic NCR^{-}ILC3s. It will be thus important to investigate if IL-23 and IL-23 responsive-ILC3s play a role in NEC pathogenesis.

In conclusion, the data presented in this study demonstrate that increased levels of IL-23 in the neonatal intestine can trigger development of Lin^{-} $ROR\gamma t^{+}Thy1^{+}Sca\text{-}1^{hi}$ ILC3s that act in concert with commensal bacteria to promote severe pathology. Thus, our results reveal a novel role for the IL-23-ILC3s axis in the pathogenesis of neonatal intestinal inflammation.

Methods

Mice

The cDNA of IL-23p19 and IL-23p40 were cloned into a pBS-Villin vector that contained a 9kb segment of the mouse villin promoter[35]. Transgenic mice were produced in the C57BL/6J background using conventional methods[49]. Identification of the transgenic *V19* mice was done by PCR amplification using the following primers: 5'-GCC AGT TTC CCT TCT TCC TC-3' and 5'- GGC TAG CAT GCA GAG ATT CC-3'. Identification of the transgenic *V40* mice was done by PCR amplification using the following primers: 5'- AAT CCA GCG CAA GAA AGA AA-3' and 5'- CAA ATG TGG TAT GGC TGA TTA TG-3'. *V19* mice crossed to *V40* mice to obtain *V23* mice. C57BL/6 , $Rorc(\gamma t)^{-/-}$, $Tcrd^{-/-}$, and $RAG1^{-/-}$ mice were purchased from The Jackson laboratory (Bar Harbor, ME). $Il\text{-}23r^{-/-}$ mice were described before [34]. Mice were maintained under specific pathogen-free conditions. All experiments involving animals were performed following guidelines of the Animal Care and Use Committee of the Icahn School of Medicine at Mount Sinai.

Flow cytometry and sorting

The small intestine, large intestine, and mesenteric lymph nodes of embryonic and P0 mice were micro-dissected using a stereo microscope and further digested with 2 mg/ml collagenase D (Roche). Cell suspension was passed through a 70-μm cell strainer and mononuclear cells were isolated. Further details and list of antibodies used have been included in Supplementary Procedures.

For the intracellular cytokine staining was measured after cells were stimulated for 6 hr with phorbol 12-myristate 13-acetate (PMA) (50 ng/ml), and ionomycin (1 μg/ml, both from Sigma-Aldrich) in the presence of monensin (2μM) (eBioscience) for the final 4 hr at 37°C culture (for details, see Supplementary Procedures).

Histology and Immunofluorescence Staining

Tissue was dissected, fixed in 10% phosphate-buffered formalin and then processed for paraffin sections. Five-micrometer sections were stained with hematoxylin and eosin. Immunofluorescence staining of frozen or paraffin-embedded tissues and list of antibodies are described in Supplementary Procedures.

Laser-capture microdissection

Frozen tissue sections (10 μm in thickness) were cut under RNase-free conditions. Samples of intestine tissue were captured from the stained slides on Arcturus CapSure Macro LCM caps by using an ArcturusXT Microdissection microscope (Applied Biosystems) (for details, see Supplementary Procedures).

DNA extraction, 16S rDNA amplification, and multiplex sequencing

DNA was obtained from whole gut of P0 mice using the DNeasy Blood and Tissue Kit (QIAGEN). Bacterial 16S rRNA genes were amplified using the primers as described in Caporaso et al. [50]. Sample preparation and analysis of 16S DNA sequence were done as previously described[51].

Barrier function assay

The barrier function assay based on sulfo-NHS-biotin was performed as described previously [43](for details, see Supplementary Procedures). Mean fluorescence intensity in the PP anlagen (WT mice) or erosive lesions (*V23* mice) and corresponding adjacent tissues were analyzed on images set to a 5% pixel saturation using ImageJ v1.49a. The data were expressed as relative fluorescence intensity representing subtraction of mean fluorescence intensity in adjacent tissue from PP anlagen (WT mice) or erosive lesions (*V23* mice).

Statistical Analysis

Differences between groups were analyzed with nonparametric Mann-Whitney test. Survival curves were analyzed by a log-rank test. All statistical analyses were performed with GraphPad Prism 5 software.

Supplementary Material

Refer to Web version on PubMed Central for supplementary material.

Acknowledgments

We thank Juan Lafaille, Daniel Mucida and Andrea Cerutti for discussions. We thank Claudia Canasto-Chibuque for help with genotyping and Parinati Kharel for help with the antibiotic treatment of mice.

We thank the Flow Cytometry, Mouse Genetics and Histology Shared Resource Facilities at Mount Sinai for technical advice and support.

This study was supported by the NIH grant P01 DK072201 and by the SUCCESS grant to S.A.L.

References

1. Oppmann B, Lesley R, Blom B, Timans JC, Xu Y, Hunte B, et al. Novel p19 protein engages IL-12p40 to form a cytokine, IL-23, with biological activities similar as well as distinct from IL-12. Immunity. 2000; 13(5):715–725. [PubMed: 11114383]
2. Ahern PP, Izcue A, Maloy KJ, Powrie F. The interleukin-23 axis in intestinal inflammation. Immunol Rev. 2008; 226:147–159. [PubMed: 19161422]
3. Ahern PP, Schiering C, Buonocore S, McGeachy MJ, Cua DJ, Maloy KJ, et al. Interleukin-23 Drives Intestinal Inflammation through Direct Activity on T Cells. Immunity. 2010; 33(2):279–288. [PubMed: 20732640]
4. Buonocore S, Ahern PP, Uhlig HH, Ivanov II, Littman DR, Maloy KJ, et al. Innate lymphoid cells drive interleukin-23-dependent innate intestinal pathology. Nature. 2010; 464(7293):1371–1375. [PubMed: 20393462]
5. Geremia A, Arancibia-Carcamo CV, Fleming MP, Rust N, Singh B, Mortensen NJ, et al. IL-23-responsive innate lymphoid cells are increased in inflammatory bowel disease. J Exp Med. 2011; 208(6):1127–1133. [PubMed: 21576383]
6. Powell N, Walker AW, Stolarczyk E, Canavan JB, Gokmen MR, Marks E, et al. The Transcription Factor T-bet Regulates Intestinal Inflammation Mediated by Interleukin-7 Receptor(+) Innate Lymphoid Cells. Immunity. 2012; 37(4):674–684. [PubMed: 23063332]
7. Cox JH, Kljavin NM, Ota N, Leonard J, Roose-Girma M, Diehl L, et al. Opposing consequences of IL-23 signaling mediated by innate and adaptive cells in chemically induced colitis in mice. Mucosal Immunol. 2012; 5(1):99–109. [PubMed: 22089030]
8. Zheng Y, Danilenko DM, Valdez P, Kasman I, Eastham-Anderson J, Wu J, et al. Interleukin-22, a T(H)17 cytokine, mediates IL-23-induced dermal inflammation and acanthosis. Nature. 2007; 445(7128):648–651. [PubMed: 17187052]
9. Hue S, Ahern P, Buonocore S, Kullberg MC, Cua DJ, McKenzie BS, et al. Interleukin-23 drives innate and T cell-mediated intestinal inflammation. Journal of Experimental Medicine. 2006; 203(11):2473–2483. [PubMed: 17030949]
10. Tait Wojno ED, Artis D. Innate lymphoid cells: balancing immunity, inflammation, and tissue repair in the intestine. Cell Host Microbe. 2012; 12(4):445–457. [PubMed: 23084914]
11. Spits H, Di Santo JP. The expanding family of innate lymphoid cells: regulators and effectors of immunity and tissue remodeling. Nat Immunol. 2011; 12(1):21–27. [PubMed: 21113163]
12. Spits H, Cupedo T. Innate lymphoid cells: emerging insights in development, lineage relationships, and function. Annu Rev Immunol. 2012; 30:647–675. [PubMed: 22224763]
13. Spits H, Artis D, Colonna M, Diefenbach A, Di Santo JP, Eberl G, et al. Innate lymphoid cells--a proposal for uniform nomenclature. Nat Rev Immunol. 2013; 13(2):145–149. [PubMed: 23348417]
14. Sun Z, Unutmaz D, Zou YR, Sunshine MJ, Pierani A, Brenner-Morton S, et al. Requirement for RORgamma in thymocyte survival and lymphoid organ development. Science. 2000; 288(5475): 2369–2373. [PubMed: 10875923]
15. Mebius RE, Rennert P, Weissman IL. Developing lymph nodes collect CD4+CD3-LTbeta+ cells that can differentiate to APC, NK cells, and follicular cells but not T or B cells. Immunity. 1997; 7(4):493–504. [PubMed: 9354470]
16. Sawa S, Cherrier M, Lochner M, Satoh-Takayama N, Fehling HJ, Langa F, et al. Lineage relationship analysis of RORgammat+ innate lymphoid cells. Science. 2010; 330(6004):665–669. [PubMed: 20929731]
17. Rankin LC, Groom JR, Chopin M, Herold MJ, Walker JA, Mielke LA, et al. The transcription factor T-bet is essential for the development of NKp46+ innate lymphocytes via the Notch pathway. Nat Immunol. 2013; 14(4):389–395. [PubMed: 23455676]

18. van de Pavert SA, Mebius RE. New insights into the development of lymphoid tissues. Nature Reviews Immunology. 2010; 10(9):664–U624.
19. Cupedo T. Human lymph node development: An inflammatory interaction. Immunol Lett. 2011; 138(1):4–6. [PubMed: 21333686]
20. Sonnenberg GF, Monticelli LA, Elloso MM, Fouser LA, Artis D. CD4(+) lymphoid tissue-inducer cells promote innate immunity in the gut. Immunity. 2011; 34(1):122–134. [PubMed: 21194981]
21. Sanos SL, Bui VL, Mortha A, Oberle K, Heners C, Johner C, et al. RORgammat and commensal microflora are required for the differentiation of mucosal interleukin 22-producing NKp46+ cells. Nat Immunol. 2009; 10(1):83–91. [PubMed: 19029903]
22. Sawa S, Lochner- M, Satoh-Takayama N, Dulauroy S, Berard M, Kleinschek M, et al. ROR gamma t(+) innate lymphoid cells regulate intestinal homeostasis by integrating negative signals from the symbiotic microbiota. Nat Immunol. 2011; 12(4):320–U371. [PubMed: 21336274]
23. Satoh-Takayama N, Vosshenrich CAJ, Lesjean-Pottier S, Sawa S, Lochner M, Rattis F, et al. Microbial Flora Drives Interleukin 22 Production in Intestinal NKp46(+) Cells that Provide Innate Mucosal Immune Defense. Immunity. 2008; 29(6):958–970. [PubMed: 19084435]
24. Marodi L. Innate cellular immune responses in newborns. Clin Immunol. 2006; 118(2-3):137–144. [PubMed: 16377252]
25. Moens E, Brouwer M, Dimova T, Goldman M, Willems F, Vermijlen D. IL-23R and TCR signaling drives the generation of neonatal Vgamma9Vdelta2 T cells expressing high levels of cytotoxic mediators and producing IFN-gamma and IL-17. J Leukoc Biol. 2011; 89(5):743–752. [PubMed: 21330350]
26. Levy O. Innate immunity of the newborn: basic mechanisms and clinical correlates. Nat Rev Immunol. 2007; 7(5):379–390. [PubMed: 17457344]
27. Kollmann TR, Crabtree J, Rein-Weston A, Blimkie D, Thommai F, Wang XY, et al. Neonatal Innate TLR-Mediated Responses Are Distinct from Those of Adults. J Immunol. 2009; 183(11): 7150–7160. [PubMed: 19917677]
28. Vanden Eijnden S, Goriely S, De Wit D, Goldman M, Willems F. Preferential production of the IL-12(p40)/IL-23(p19) heterodimer by dendritic cells from human newborns. Eur J Immunol. 2006; 36(1):21–26. [PubMed: 16342235]
29. Willems F, Vollstedt S, Suter M. Phenotype and function of neonatal DC. Eur J Immunol. 2009; 39(1):26–35. [PubMed: 19137537]
30. Vanden Eijnden S, Goriely S, De Wit D, Willems F, Goldman M. IL-23 up-regulates IL-10 and induces IL-17 synthesis by polyclonally activated naive T cells in human. Eur J Immunol. 2005; 35(2):469–475. [PubMed: 15682457]
31. Sun CM, Fiette L, Tanguy M, Leclerc C, Lo-Man R. Ontogeny and innate properties of neonatal dendritic cells. Blood. 2003; 102(2):585–591. [PubMed: 12663436]
32. Dakic A, Shao QX, D'Amico A, O'Keeffe M, Chen WF, Shortman K, et al. Development of the dendritic cell system during mouse ontogeny. J Immunol. 2004; 172(2):1018–1027. [PubMed: 14707075]
33. Parham C, Chirica M, Timans J, Vaisberg E, Travis M, Cheung J, et al. A receptor for the heterodimeric cytokine IL-23 is composed of IL-12Rbeta1 and a novel cytokine receptor subunit, IL-23R. J Immunol. 2002; 168(11):5699–5708. [PubMed: 12023369]
34. Awasthi A, Riol-Blanco L, Jager A, Korn T, Pot C, Galileos G, et al. Cutting edge: IL-23 receptor gfp reporter mice reveal distinct populations of IL-17-producing cells. J Immunol. 2009; 182(10): 5904–5908. [PubMed: 19414740]
35. Pinto D, Robine S, Jaisser F, El Marjou F, Louvard D. Regulatory sequences of the mouse villin gene that efficiently drive transgenic expression in immature and differentiated epithelial cells of small and large intestines. J Biol Chem. 1999; 274(10):6476–6482. [PubMed: 10037740]
36. Uhlig HH, McKenzie BS, Hue S, Thompson C, Joyce-Shaikh B, Stepankova R, et al. Differential activity of IL-12 and IL-23 in mucosal and systemic innate immune pathology. Immunity. 2006; 25(2):309–318. [PubMed: 16919486]
37. Crellin NK, Trifari S, Kaplan CD, Satoh-Takayama N, Di Santo JP, Spits H. Regulation of cytokine secretion in human CD127(+) LTi-like innate lymphoid cells by Toll-like receptor 2. Immunity. 2010; 33(5):752–764. [PubMed: 21055975]

38. Mueller SN, Hosiawa-Meagher KA, Konieczny BT, Sullivan BM, Bachmann MF, Locksley RM, et al. Regulation of homeostatic chemokine expression and cell trafficking during immune responses. Science. 2007; 317(5838):670–674. [PubMed: 17673664]
39. Marchesi F, Martin AP, Thirunarayanan N, Devany E, Mayer L, Grisotto MG, et al. CXCL13 expression in the gut promotes accumulation of IL-22-producing lymphoid tissue-inducer cells, and formation of isolated lymphoid follicles. Mucosal Immunol. 2009; 2(6):486–494. [PubMed: 19741597]
40. Mebius RE. Organogenesis of lymphoid tissues. Nat Rev Immunol. 2003; 3(4):292–303. [PubMed: 12669020]
41. Eberl G, Marmon S, Sunshine MJ, Rennert PD, Choi Y, Littman DR. An essential function for the nuclear receptor RORgamma(t) in the generation of fetal lymphoid tissue inducer cells. Nat Immunol. 2004; 5(1):64–73. [PubMed: 14691482]
42. Vonarbourg C, Mortha A, Bui VL, Hernandez PP, Kiss EA, Hoyler T, et al. Regulated expression of nuclear receptor RORgammat confers distinct functional fates to NK cell receptor-expressing RORgammat(+) innate lymphocytes. Immunity. 2010; 33(5):736–751. [PubMed: 21093318]
43. Lei Z, Maeda T, Tamura A, Nakamura T, Yamazaki Y, Shiratori H, et al. EpCAM contributes to formation of functional tight junction in the intestinal epithelium by recruiting claudin proteins. Dev Biol. 2012; 371(2):136–145. [PubMed: 22819673]
44. Sonnenberg GF, Monticelli LA, Alenghat T, Fung TC, Hutnick NA, Kunisawa J, et al. Innate lymphoid cells promote anatomical containment of lymphoid-resident commensal bacteria. Science. 2012; 336(6086):1321–1325. [PubMed: 22674331]
45. Philip NH, Artis D. New friendships and old feuds: relationships between innate lymphoid cells and microbial communities. Immunol Cell Biol. 2013; 91(3):225–231. [PubMed: 23337700]
46. Maloy KJ, Salaun L, Cahill R, Dougan G, Saunders NJ, Powrie F. CD4+CD25+ T(R) cells suppress innate immune pathology through cytokine-dependent mechanisms. J Exp Med. 2003; 197(1):111–119. [PubMed: 12515818]
47. Coursodon-Boyiddle CF, Snarrenberg CL, Adkins-Rieck CK, Bassaganya-Riera J, Hontecillas R, Lawrence P, et al. Pomegranate seed oil reduces intestinal damage in a rat model of necrotizing enterocolitis. Am J Physiol Gastrointest Liver Physiol. 2012; 303(6):G744–751. [PubMed: 22821948]
48. Fox JG, Ge Z, Whary MT, Erdman SE, Horwitz BH. Helicobacter hepaticus infection in mice: models for understanding lower bowel inflammation and cancer. Mucosal Immunol. 2011; 4(1): 22–30. [PubMed: 20944559]
49. Shang L, Fukata M, Thirunarayanan N, Martin AP, Arnaboldi P, Maussang D, et al. Toll-like receptor signaling in small intestinal epithelium promotes B-cell recruitment and IgA production in lamina propria. Gastroenterology. 2008; 135(2):529–538. [PubMed: 18522803]
50. Caporaso JG, Kuczynski J, Stombaugh J, Bittinger K, Bushman FD, Costello EK, et al. QIIME allows analysis of high-throughput community sequencing data. Nat Methods. 2010; 7(5):335–336. [PubMed: 20383131]
51. Bongers G, Pacer ME, Geraldino TH, Chen L, He Z, Hashimoto D, et al. Interplay of host microbiota, genetic perturbations, and inflammation promotes local development of intestinal neoplasms in mice. J Exp Med. 2014; 211(3):457–472. [PubMed: 24590763]

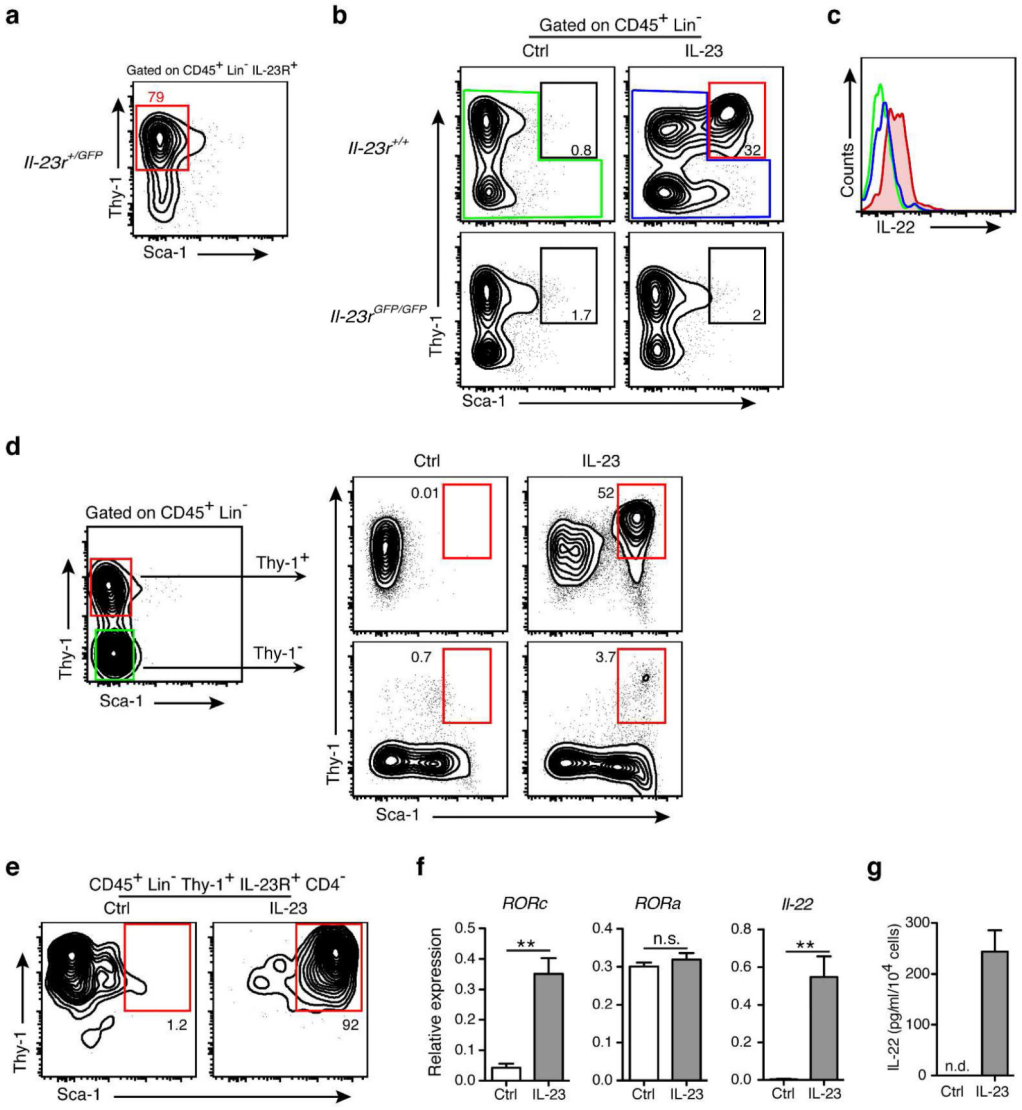

Figure 1. IL-23 promotes development of Thy1^{+}Sca-1^{hi} ILCs *in vitro*

(**a**) Flow cytometric analysis of Thy1 and Sca-1 expression of gated CD45^{+}Lin^{-}IL-23R^{+} cells from the intestine of *Il-23r*$^{+/GFP}$ mice at embryonic day E18.5. (**b**) *In vitro* stimulated CD45^{+}Lin^{-} leukocyte subpopulations from the intestine of *Il-23r*$^{+/+}$ and *Il-23r*$^{GFP/GFP}$ mice at embryonic day E18.5 with IL-23 (10ng/ml) or vehicle control for 72 hr. Representative flow cytometry plots showing CD45^{+}Lin^{-}Thy1^{+}Sca-1^{hi} population after culture. (**c**) Intracellular cytokine stain of IL-22 expression by the populations shown in (**b**), colors correspond to the populations analyzed. (**d**) Culture of sorted Lin^{-}Thy1^{+} and Lin^{-}Thy1^{-} cells from the wild-type intestine at embryonic day E18.5 respond to IL-23 (10ng/ml) or vehicle (Ctrl) stimulation after 72 hr. Representative flow cytometry plots showing CD45^{+}Lin^{-}Thy1^{+}Sca-1^{hi} population after culture. (**e**) Representative flow cytometry plots showing sorted Lin^{-}Thy1^{+}IL-23R^{+}CD4^{-} cells from the intestine of *Il-23r*$^{+/GFP}$ mice at embryonic day E18.5 respond to IL-23 (10ng/ml) or vehicle (Ctrl) stimulation after 72 hr. (**f**) Quantitative RT-PCR analysis of *Il-22*, *Rorc* and *Rora* mRNA expression in the Lin-Thy1^{+}IL-23R^{+}CD4^{-} cells stimulated with control media (Ctrl) or

IL-23. NS, not significant. ** $P < 0.01$. (**g**) ELISA evaluation of IL-22 in the culture supernatant of the $Lin^{-}Thy1^{+}IL\text{-}23R^{+}CD4^{-}$ cells stimulated with control media (Ctrl) or IL-23. Data are shown as means ± s.e.m., n = 3–5 per group. ND, not detectable. Results are representative of three independent experiments.

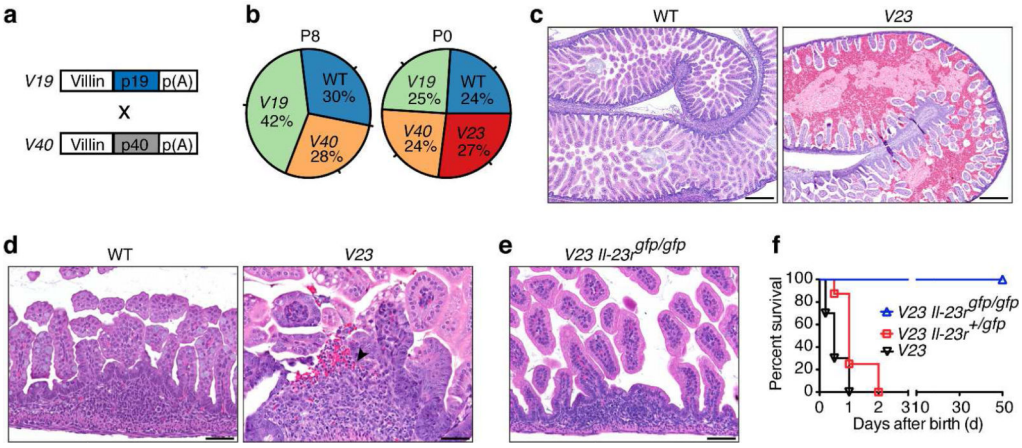

Figure 2. Transgenic expression of IL-23 in the intestine causes formation of erosive lesions, bleeding, and neonatal death

(**a**) Scheme for generation of *V23* mice. Independent sets of murine villin promoter (9kb)-driven transgenes encoding IL-23p19 or p40 were used to generate *V19* and *V40* mice, respectively. (**b**) Genotypic ratios of WT, *V19*, *V40* and *V23* mice at different ages P0 (n = 97) and P8 (n = 69). (**c** and **d**) Representative H&E stained sections of the small intestine of WT and *V23* mice at P0. Scale bars, 250 μm in (**c**) and 50 μm in (**d**). Arrow indicates an erosive lesion. (**e**) Representative H&E stained section of the small intestine of *V23 Il-23r*$^{GFP/GFP}$ mice at P0. Scale bars, 50 μm. (**f**) The survival curves of *V23* (n=16), *V23 Il-23r*$^{+/GFP}$ (n=15), and *V23 Il-23r*$^{GFP/GFP}$ (n=18) mice. $P < 0.001$ between *V23 Il-23r*$^{GFP/GFP}$ and *V23* mice by Log-rank test. Results are representative of three independent experiments.

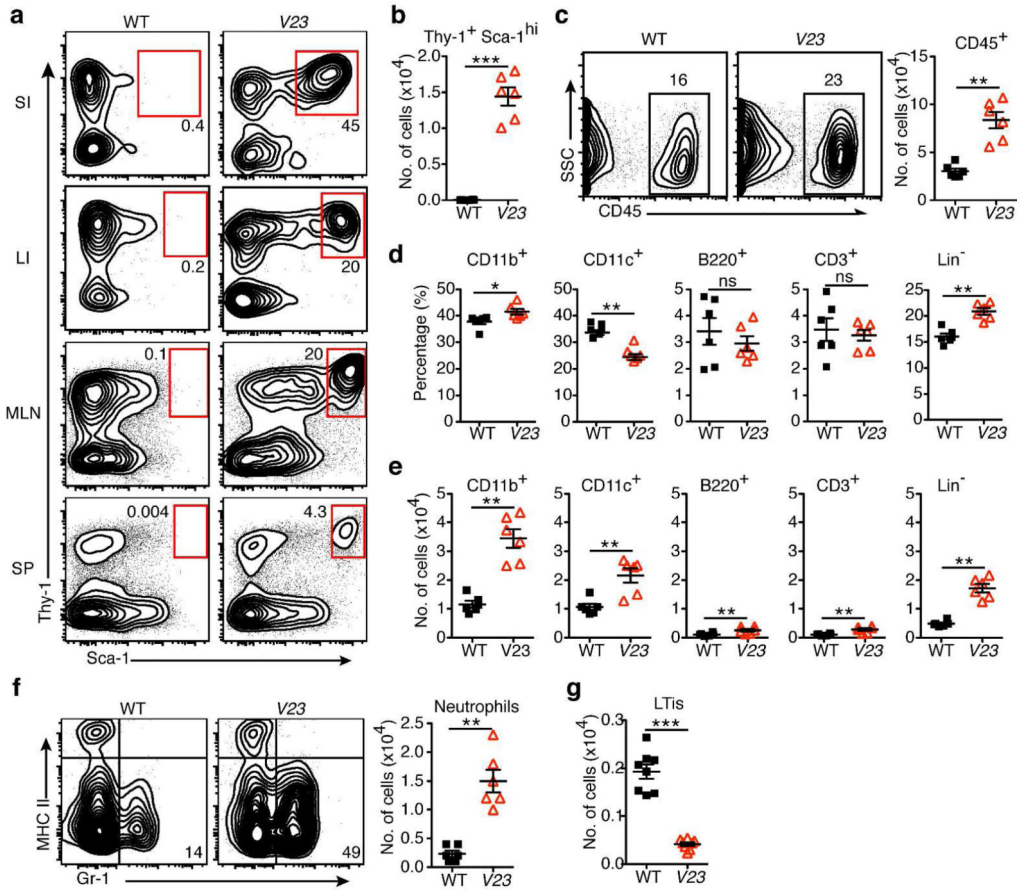

Figure 3. Gut-specific expression of IL-23 activated and expanded Thy1^{+}Sca-1^{hi} ILC3s in the neonatal intestine

(**a**) Relative number of Lin^{-}Thy1^{+}Sca-1^{hi} cells in small intestine (SI), large intestine (LI), mesenteric lymph nodes (MLN) and spleen (SP) of WT and *V23* mice at P0. Representative flow cytometry plots gated on CD45^{+}Lin^{-}. (**b**) Absolute number of Lin^{-}Thy1^{+}Sca-1^{hi} cells in the small intestine of WT and *V23* mice at P0. Means ± s.e.m., n = 5–6 per group, ***P < 0.001. (**c**) Relative (left) and absolute (right) number of CD45^{+} cells in the small intestine of WT and *V23* mice at P0. Dot plots show cells gated on live cells. Means ± s.e.m., n = 5–6 per group, ** P < 0.01. (**d** and **e**) Relative (**d**) and absolute (**e**) number of CD11b^{+}, CD11c^{+}, CD3^{+}, B220^{+} and Lin^{-} cells in the small intestine of WT and *V23* mice at P0. Means ± s.e.m., n = 5–6 per group. NS, not significant, * P < 0.05, ** P < 0.01, ***P < 0.001. (**f**) Relative (left) and absolute (right) number of CD45^{+}CD11b^{+}MHCII^{-}Gr-1^{+} cells in the small intestine of WT and *V23* mice at P0. Dot plots show cells gated on CD45^{+}CD11b^{+}. Means ± s.e.m., n = 5–6 per group, ** P < 0.01. (**g**) Absolute number of LTi cells (Lin^{-}CD4^{+}) in the small intestine of WT and *V23* mice at P0. Means ± s.e.m., n = 7–8 per group, ***P < 0.001. Data are representative of three independent experiments.

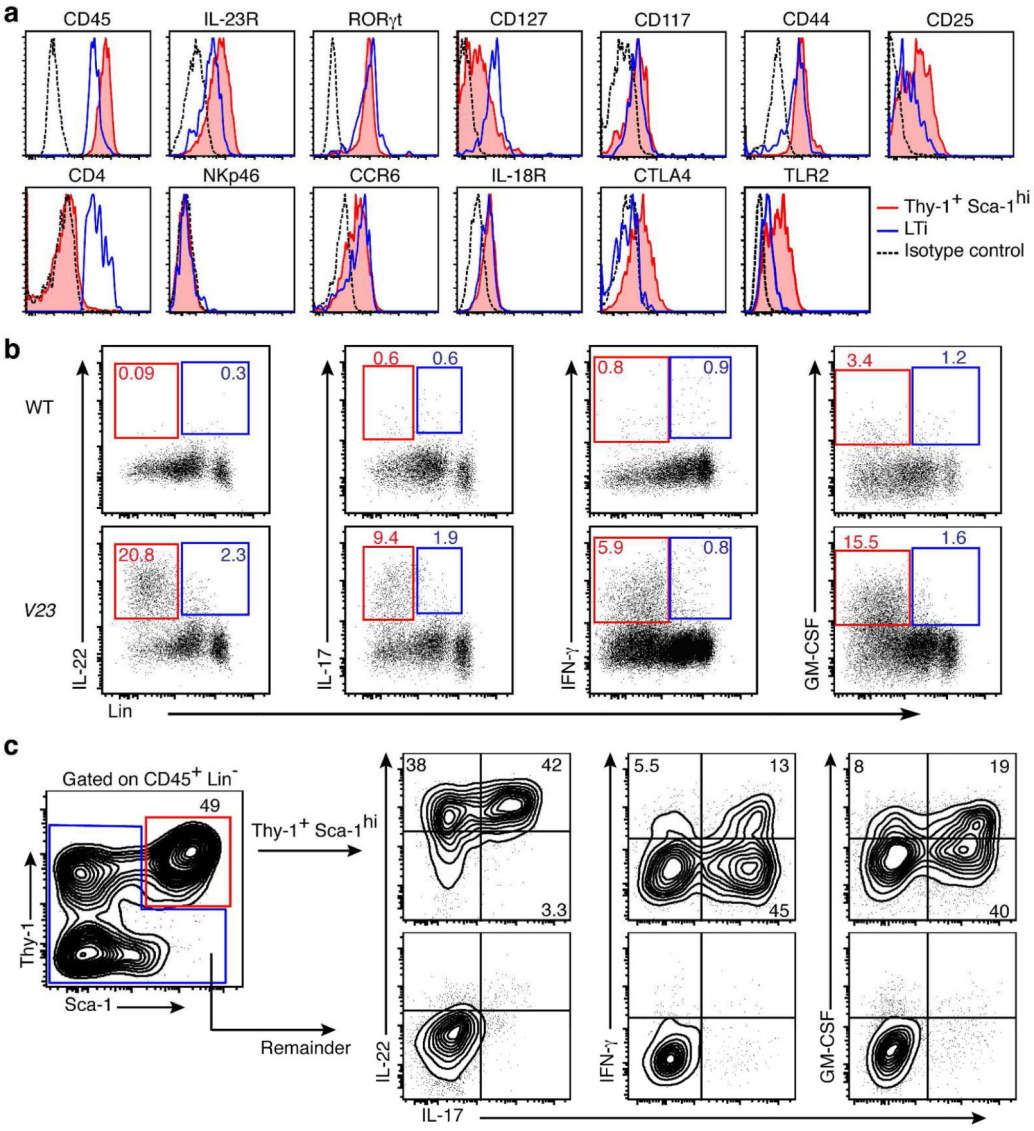

Figure 4. Thy1^{+}Sca-1^{hi} cells in the intestine of the *V23* mice are NCR^{-}ILC3s

(**a**) Phenotype of lineage-negative (Lin^{-}, CD3^{-}B220^{-}CD11b^{-}Gr-1^{-}Ter119^{-}) Thy1^{+}Sca-1^{hi} cells. Histograms are electronically gated on Lin^{-} cells. Red lines indicate Lin^{-}Thy1^{+}Sca-1^{hi} ILC3, blue lines denote LTi cells (Lin^{-}CD4^{+}), and dotted black lines indicate isotype controls. (**b**) Expression of indicated cytokines analyzed by flow cytometry on the CD45^{+}Lin^{+} and CD45^{+}Lin^{-} populations after stimulation with phorbol 12-myristate 13-acetate (PMA) and ionomycin. Dot plots show cells gated on CD45^{+}. Outlines areas in red indicate Lin^{-} and outlines areas in blue indicate Lin^{+}. (**c**) Intracellular cytokine expression by Lin^{-}Thy1^{+}Sca-1^{hi} cells (red) in comparison with remaining cells (blue) from the small intestine of *V23* mice at P0 following stimulation with PMA and ionomycin. Data are representative of at least three independent experiments.

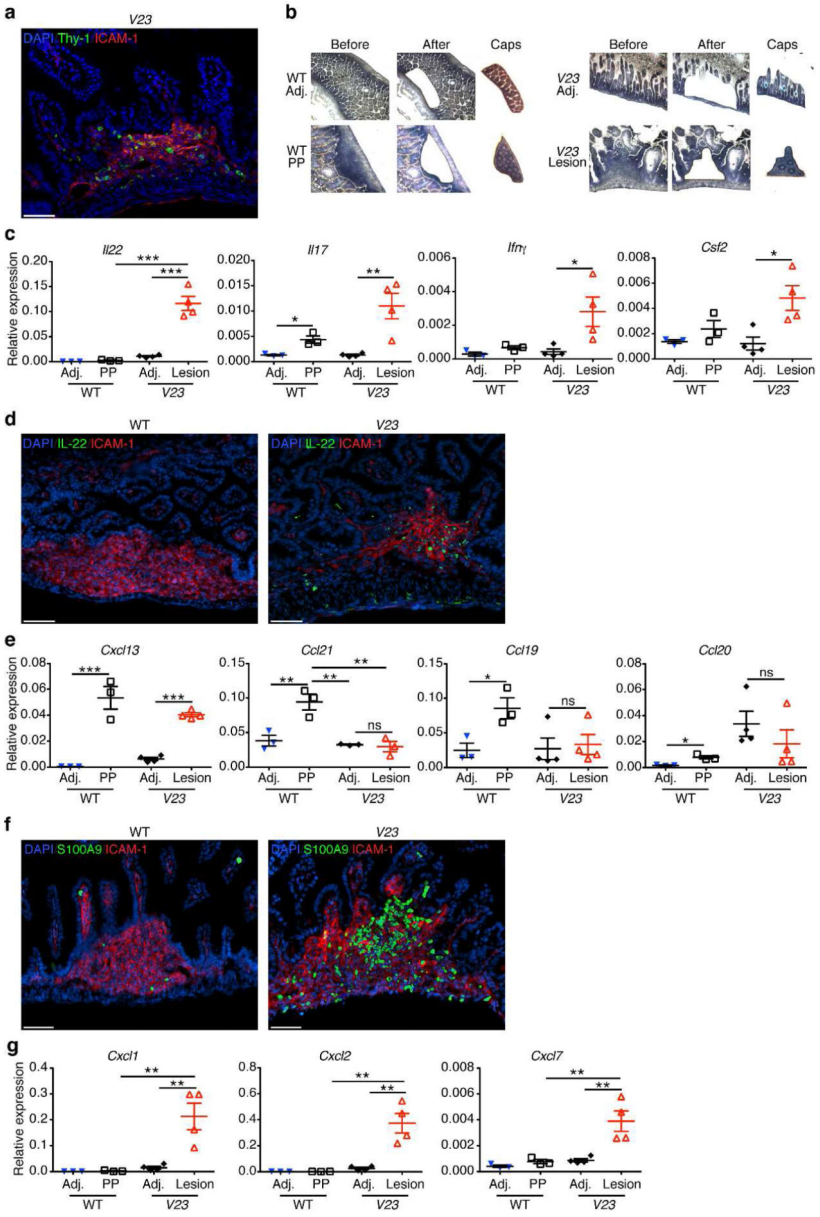

Figure 5. Thy1^{+}Sca-1^{hi} ILC3s are located within erosive lesions in the intestine

(**a**) Immunofluorescence staining of the small intestine at P0 showing the presence of Thy1^{+} cells in ICAM^{+} cells aggregates in *V23* mice (Thy1, green; ICAM-1, red; cell nuclei, DAPI). Scale bars, 50μm. (**b**) Histology of snap-frozen small intestine from WT and *V23* mice. Slides show tissue before (left), after (middle) laser microdissection, as well as excised tissue in caps (right). (**c**) Cytokine expression measured by quantitative RT-PCR in microdissected Peyer's patches anlagen (PP)/erosive lesions areas (Lesion) and adjacent control areas (Adj) isolated from P0 WT and *V23* mice. Means ± s.e.m., n = 4 per group. * $P < 0.05$, ** $P < 0.01$, ***$P < 0.001$. (**d**) Immunofluorescence staining of the small intestine of *V23* mice at P0 showing the presence of IL-22^{+} cells within ICAM^{+} aggregates (IL-22, green; ICAM-1, red; cell nuclei, DAPI). Scale bars, 50μm. (**e**) Chemokine expression in microdissected Peyer's patches anlagen (PP)/erosive lesions areas (Lesion) and adjacent

control areas (Adj) isolated from P0 WT and *V23* mice. Means ± s.e.m., n = 4 per group. NS, not significant, * $P < 0.05$, ** $P < 0.01$, *** $P < 0.001$. (**f**) Immunofluorescence staining the small intestine at P0 showing the presence of neutrophils ($S100A9^+$) in $ICAM^+$ cells aggregates (S100A9, green; ICAM-1, red; cell nuclei, DAPI). Scale bars, 50μm. (**g**) Expression of neutrophil chemoattracting chemokines in microdissected Peyer's patches anlagen (PP)/erosive lesions areas (Lesion) and adjacent control areas (Adj) isolated from P0 WT and *V23* mice. Means ± s.e.m., n = 4 per group, * * $P < 0.01$.

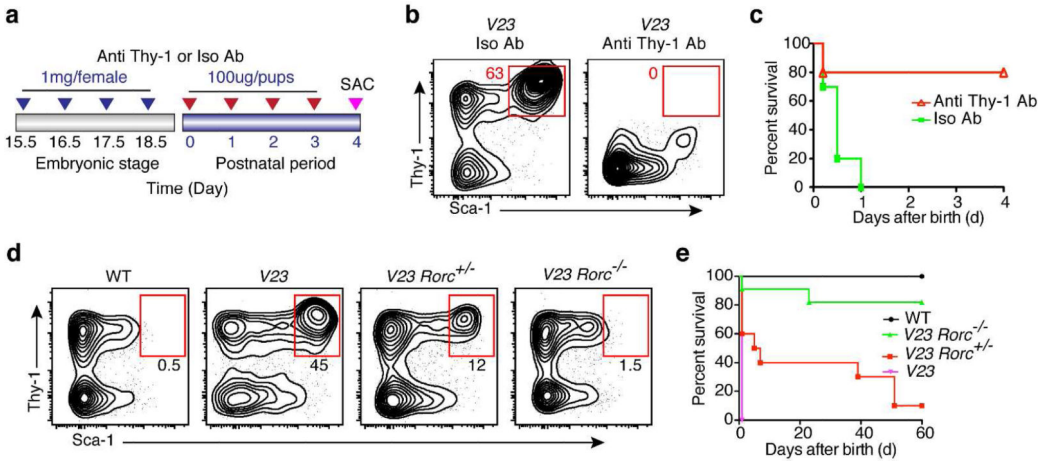

Figure 6. Thy1^{+}Sca-1^{hi} ILC3s are the main drivers of the intestinal pathogenesis

(**a**) Protocol used for *in vivo* depletion of Thy1^{+} cells in newborn *V23* mice. The pregnant mothers were administered intravenously with 1 mg rat anti-Thy1 mAb or 1 mg isotype control mAb at gestational days 15.5, 16.5, 17.5 and 18.5. After birth pups were injected i.p. daily with 100 μg anti-Thy1 mAb or 100 μg isotype control per mouse for 4 days. (**b**) Flow cytometric analysis of the Lin^{-}Thy1^{+}Sca-1^{hi} population in the small intestine after antibody injection. Dot plots show cells gated on CD45^{+}Lin^{-}. (**c**) Survival curves of *V23* pups treated with anti-Thy1 (n = 12) or isotype (n = 12). ** $P < 0.01$ between groups by Log-rank test. (**d**) Flow cytometry plot showing the proportion of Lin^{-}Thy1^{+}Sca-1^{hi} cells in the small intestine of *V23*, *V23Rorc(γt)*$^{+/-}$, and *V23Rorc(γt)*$^{-/-}$ mice at P0. Dot plots show cells gated on CD45^{+}Lin^{-}. (**e**) Survival curves of *V23* (n = 15), *V23Rorc(γt)*$^{+/-}$ (n = 18), and *V23Rorc(γt)*$^{-/-}$ (n = 22) mice. *** $P < 0.001$ between *V23Rorc(γt)*$^{+/-}$ /*V23Rorc(γt)*$^{-/-}$ mice and *V23* mice by Log-rank test. Data are representative of three independent experiments.

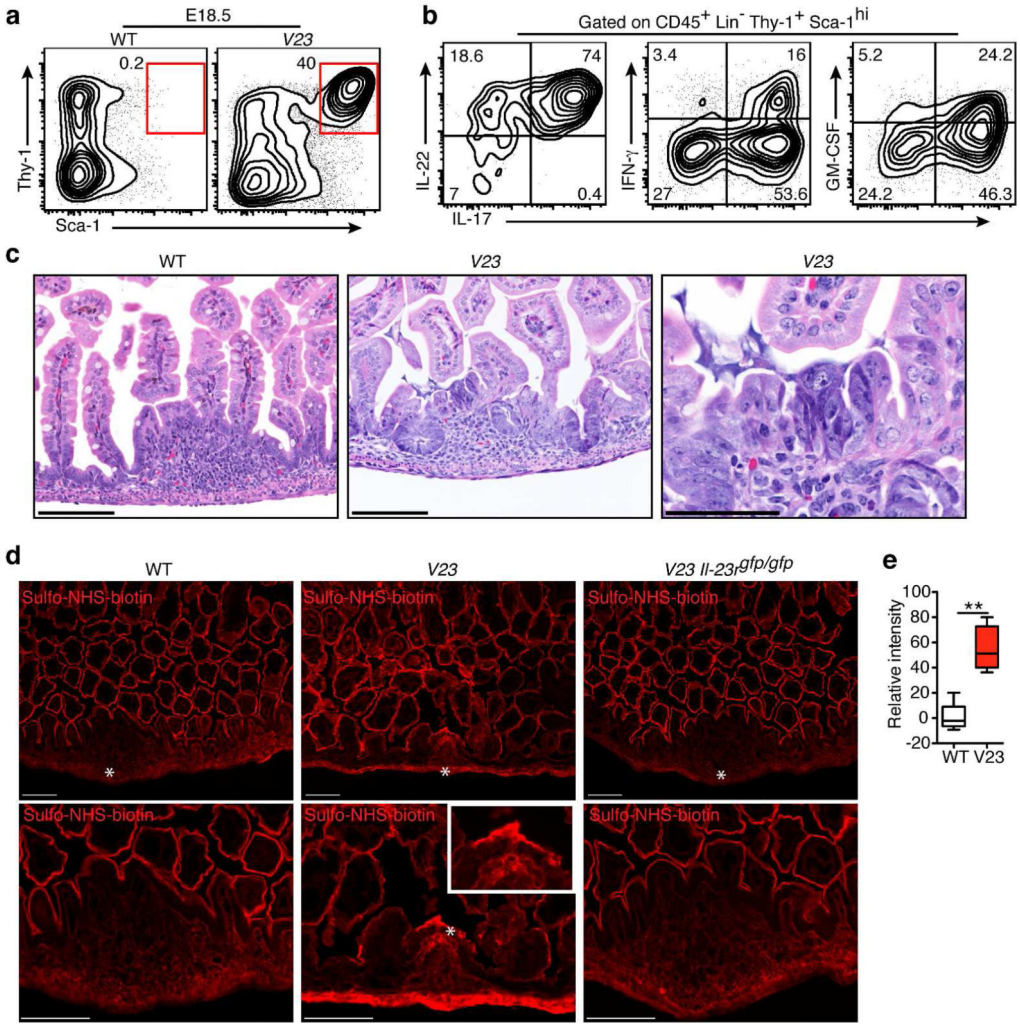

Figure 7. Intestinal Thy1^{+}Sca-1^{hi} ILCs dysregulate epithelial permeability at prenatal stage

(**a**) Flow cytometric analysis of the Lin^{-}Thy1^{+}Sca-1^{hi} cells in the small intestine of mice at embryonic day E18.5. Dot plots show cells gated on CD45^{+}Lin^{-}. (**b**) Representative cytokine expression profile of Lin^{-}Thy1^{+}Sca-1^{hi} ILC3s present in the small intestine of embryonic *V23* mice (E18.5). (**c**) Representative H&E stained sections of the small intestine of WT and *V23* embryo mice (E18.5). Scale bars, 100 μm. (**d**) The fluorescence staining of proteins labeled with sulfo-NHS-biotin in the small intestine after injection of the probe into the lumen of the intestine of embryos at E18.5. Stars indicate cellular aggregates in the gut. Scale bars, 100μm. Zoomed-in boxed area shows fluorescence staining of cellular aggregates in *V23* mice. Data are representative of three independent experiments. (**e**) Quantification of relative fluorescent intensity in the PP anlagen of WT mice (2-5 sections for each mouse) and in erosive lesions of *V23* mice (4-10 sections for each mouse). Data are shown as means ± s.e.m. of n = 5 mice per group. $^{**}P < 0.01$, nonparametric Mann-Whitney test.

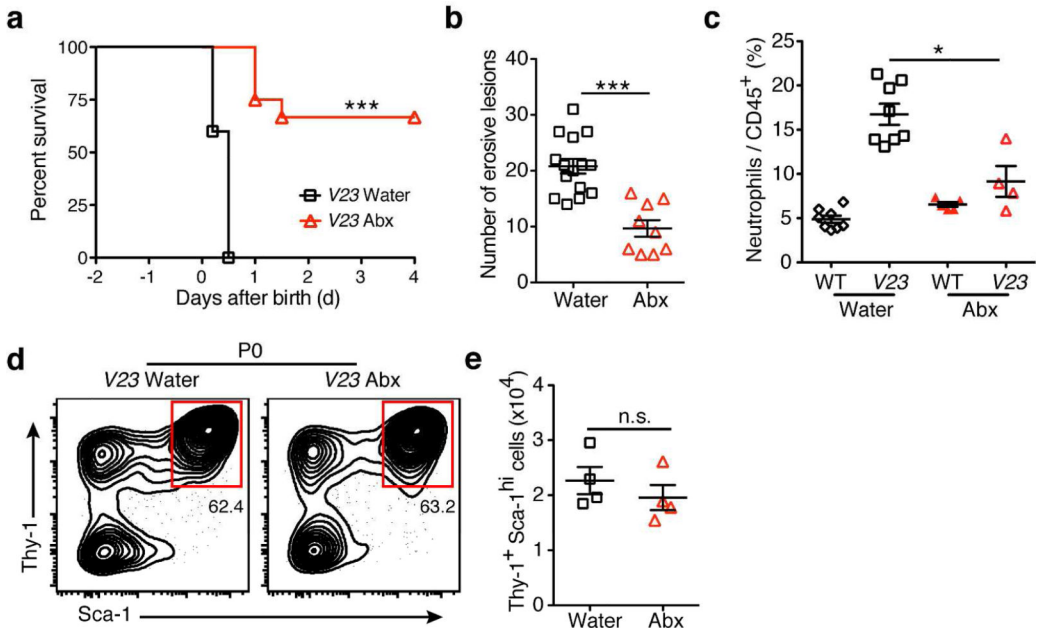

Figure 8. Commensal bacteria aggravate intestinal pathology induced by Thy1^{+}Sca-1^{hi} ILCs

(**a**) Survival curves of *V23* mice derived from mothers treated with (n=22) or without (n=15) an antibiotic cocktail in drinking water during pregnancy. ***, $P < 0.001$ (Log-rank test). (**b**) Number of erosive lesions in the intestine of *V23* mice born from mothers receiving water or antibiotic. Data are shown as means ± s.e.m., n = 10-15 for each group, ***, $P < 0.001$. (**c**) Relative number of neutrophils (CD11b^{+}Gr-1^{+}) in the small intestine of *V23* mice born from mothers receiving water or antibiotic. Data are shown as means ± s.e.m., n = 4–8 per group, * $P < 0.05$. (**d** and **e**) Relative (**d**) and absolute (**e**) number of the Lin^{-}Thy1^{+}Sca-1^{hi} cells in the small intestine of *V23* mice born from mothers receiving water or antibiotic. Data are shown as means ± s.e.m., n=4 for each group. Dot plots show cells gated on CD45^{+}Lin^{-}. NS, not significant.